

Characteristic Measurement of Loudspeaker Using Large Area Radiation Panel for Generating Inclined Sound Field

傾斜音場を生成する大面積放射パネルを用いたスピーカの特性計測

Shotaro Daito^{1,‡}, Naoto Wakatsuki¹, Tadashi Ebihara¹, Keiichi Zempo¹, and Koichi Mizutani¹ (1Univ. Tsukuba)

大東祥太郎^{1,‡}, 若槻尚斗^{1,2}, 海老原格^{1,2}, 善甫啓一^{1,2}, 水谷孝一^{1,2} (1 筑波大院・シス情工, 2 筑波大・シス情系)

1. Introduction

Audio guidance in public spaces has been attracting attention as a information presentation that is not dependent on vision [1]. Auditory guidance using the direction of arrival of the sound can provide people the guiding direction intuitively. Hence, a loudspeaker that can indicate the guiding direction regardless of position on a pathway is necessary. To meet such demand, we have proposed a panel loudspeaker that radiates sound with an inclined angle from a flexural wave propagating in an elastic plate (hereafter, we call this “inclined sound”) [2],[3]. Hence, if we can cover a ceiling of corridors with large panel speakers, To indicate the guiding direction regardless of position on a pathway would be achieved [4]. this loudspeaker was suggested a numerical analysis method for the propagation properties of flexural wave in honeycomb sandwich panel [5]. We studied the wave propagation characteristics and the reflection characteristics in honeycomb sandwich panel [6],[7]. In the process, we needed to investigate the acoustic characteristics as the panel loudspeaker. Hence, in this study, we build the panel loudspeaker actually and examine the sound radiation characteristics to measure the sound field generated by the panel loudspeaker.

2. The panel loudspeaker

The panel loudspeaker is composed of a honeycomb sandwich panel, an acoustic material, and an enclosure as shown in Fig. 1. The dimension of the honeycomb sandwich panel is $2240 \times 120 \times 23$ (mm³). The panel is made of aluminum. The sound absorbing material is for suppressing the sound radiated by back side of the panel. The sound absorbing material is made of needle-felted fabrics. The enclosure is for reducing low frequency interference between front side and back side of the panel. The enclosure is made of wood. In order to keep the honeycomb panel close to free edge boundary condition, a rubber sheet was set between the panel and the enclosure. In this study, the panel loudspeaker is driven by an electro-magnetic exciter

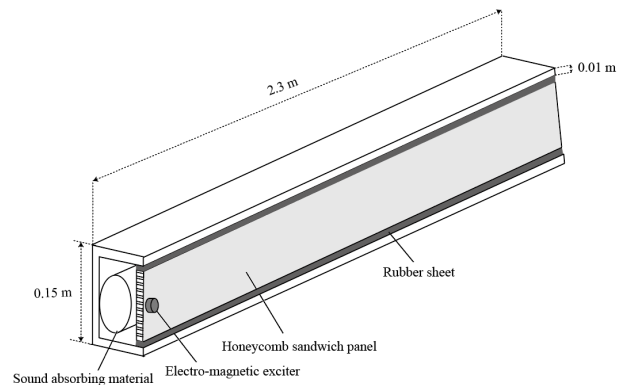


Fig. 1 The structure of the panel loudspeaker.

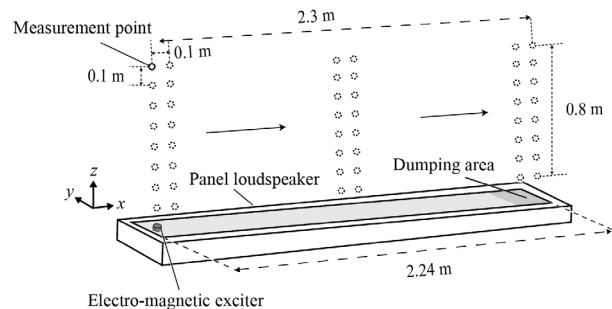


Fig. 2 Experimental setup of the sound field measurement in the panel loudspeaker.

on front side of the panel.

3. Measurement

In this study, the sound field generated by the panel speaker is measured experimentally using a sound intensity probe. The sound intensity probe is composed of four microphones arranged on a regular tetrahedron. The average sound pressure p and the product of the sound pressure differential approximation dp_x, dp_y, dp_z in the x, y, z -axis direction and the infinitesimal displacement dl is obtained using the following equations:

$$p = \frac{1}{4}(p_1 + p_2 + p_3 + p_4) \quad (1)$$

$$dl * dp_x = \frac{1}{4}(-\sqrt{2}p_1 + 2\sqrt{2}p_2 - \sqrt{2}p_3) \quad (2)$$

$$dl * dp_y = \frac{1}{4}(-\sqrt{6}p_1 + \sqrt{6}p_3) \quad (3)$$

$$dl * dp_z = \frac{1}{4}(p_1 + p_2 + p_3 - 3p_3) \quad (4)$$

where p_1, p_2, p_3, p_4 are respectively the sound pressure at four microphones. The cross power spectrum P_i of p and $dl * dp_i$ ($i = x, y, z$) is expressed as $P_i = \mathcal{F}[R_i]$ using the cross-correlations R_i of p with $dl * dp_i$. ($\mathcal{R}e[P_x], \mathcal{R}e[P_y], \mathcal{R}e[P_z]$) represents the sound field generated by the panel loudspeaker.

Figure 2 shows experimental setup of the sound field measurement in the panel loudspeaker. One end of the panel was driven by an electromagnetic exciter. Input signal. The input signal was a linear chirp signal from 0 to 24 (kHz) for a period of 8 (s). The signals received by the sound intensity probe were sampled at 48 (kHz) by an analog-to-digital converter (NI USB-6212). The measurement range in x -axis direction was from 0 to 2.3 (m) and the measurement range in z -axis direction was from 0.1 to 0.8 (m). The sound intensity probe was scanned at 0.1 (m) intervals along x and z -axis by single axis translation stage. The opposite end of the panel was damped by clay to reduce reflections.

We compared between experimental and theoretical results. Figure 3 shows the sound field generated by the panel loudspeaker at 0.8 – 1.0, 1.8 – 2.0 (kHz) in z - x plane. Each arrows in Fig. 3 is the unit vector of sound direction and color map shows sound pressure distribution. In Fig. 3(a), the radiation angle with respect to the x -axis at $x = 1.0 - 2.0, z = 0.2 - 0.8$ (m) was 0.67 – 0.93 (rad). And, the radiation angle in Fig. 3(b) was 0.83 -1.0 (rad). Figure 4 shows theoretical and simulated radiation angles in the previous study [5]. The theoretical radiation angle at 1.0, 2.0 (kHz) were 0.7, 0.8 (rad). This result suggests the panel loudspeaker radiates sound with theoretical angles in error range of 0.03 – 0.2 (rad). And the sound pressure generated by the panel speaker is approximately equal in a range of 0.8m.

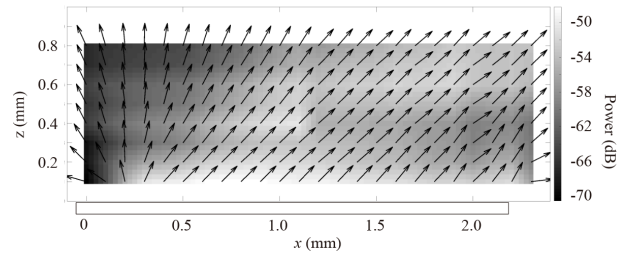
4. Conclusion

We measured the sound field generated by the panel speaker using a sound intensity probe. As the results, it was confirmed the panel loudspeaker radiates sound with theoretical angles in error range of 0.03 – 0.2 (rad). In the future, the measurement of the amplitude distribution on the panel loudspeaker is planned to analyze damping characteristics of the flexural wave on the panel loudspeaker.

Acknowledgment

This work was partly supported by JSPS

(a) Frequency: 0.8-1.0 (kHz)



(b) Frequency: 1.8-2.0 (kHz)

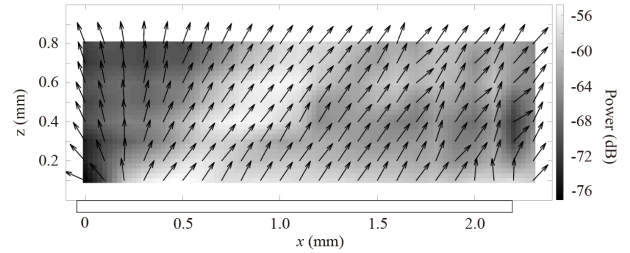


Fig. 3 the sound field generated by the panel loudspeaker

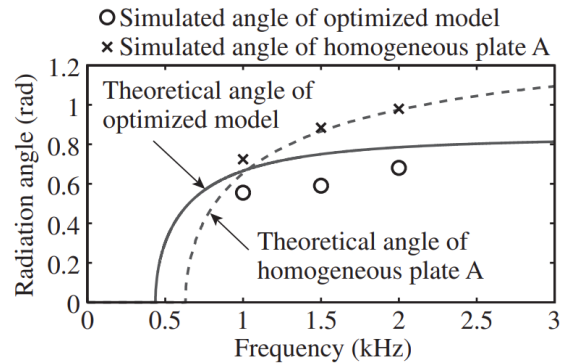


Fig. 4 Theoretical and simulated radiation angles in the previous study [5].

KAKENHI Grant Number 17K06222 and 20H04202.

References

1. J. Tardieu, P. Susini, F. Poisson, H. Kawakami, and S. McAdams. *Applied Acoustics*, (2009), Vol. 70, No. 9, p.1183 – 1193.
2. A. Fujii, N. Wakatsuki, and K. Mizutani, *Proc. the 35th Symposium on Ultrasonic Electronics*, (2014), p. 403
3. A. Fujii, N. Wakatsuki, and K. Mizutani: *Procs. 20th Int. Congr. Sound and Vib. (ICSV20)*, (2013), R25-344.
4. N. Wakatsuki, and K. Mizutani, T. Ebihara, H. Kinoshita, and A. Fujii: *Procs. 25th Int. Congr. Sound and Vib. (ICSV25)*, (2018), 1021 1-5.
5. A. Fujii, N. Wakatsuki, and K. Mizutani, *Japanese J. Appl. Phys.*, 54, (2015), 07HB08.
6. S. Daito, N. Wakatsuki, and K. Mizutani, T. Ebihara, *Proc. the 35th Symposium on Ultrasonic Electronics*, 2019, 3P1-5.
7. S. Daito, N. Wakatsuki, and K. Mizutani, T. Ebihara, *Proc. the 36th Symposium on Ultrasonic Electronics*, 2020, 2Pa1-1.